Published in final edited form as:
J Neurophysiol. 2008 April ; 99(4): 1643–1652. doi:10.1152/jn.01253.2007.

Summation of Excitatory and Inhibitory Synaptic Inputs by Motoneurons With Highly Active Dendrites

Allison S. Hyngstrom[1], **Michael D. Johnson**[1], and **C. J. Heckman**[1,2]

[1]Department of Physiology, Northwestern University, Chicago, Illinois

[2]Department of Physical Medicine and Rehabilitation, Northwestern University, Chicago, Illinois

Abstract

We investigated summation of steady excitatory and inhibitory inputs in spinal motoneurons using an in vivo preparation, the decerebrate cat, in which neuromodulatory input from the brain stem facilitated a strong persistent inward current (PIC) in dendritic regions. This dendritic PIC amplified both excitatory and inhibitory synaptic currents two-to threefold, but within different voltage ranges. Amplification of excitatory synaptic current peaked at voltage-clamp holding potentials near spike threshold (about −55 to −50 mV), whereas amplification of inhibitory current peaked at significantly more depolarized levels (about −45 to −40 mV). Thus the linear sum of excitatory and inhibitory currents tended to vary from net excitatory to net inhibitory as holding potential was depolarized. The actual summed currents, however, diverged from the predicted linear currents. At the peak of excitation, summation averaged about 15% sublinear (actual sum was less positive than the linear sum). In contrast, at the peak of inhibition, summation averaged about 18% supralinear (actual more positive than linear). Moreover, these nonlinear effects were substantially larger in cells where the variation from peak excitation to peak inhibition for linear summation was larger. When descending neuromodulatory input was eliminated by acute spinalization, PIC amplification was not observed and summation tended to be either sublinear or approximately linear, depending on input source. Overall, in cells with strong PICs, nonlinear summation of excitation and inhibition does occur, but this nonlinearity results in a more consistent relationship between membrane potential and the summed excitatory and inhibitory current.

Introduction

Many types of neurons have voltage-sensitive conductances distributed throughout their dendritic trees (Gulledge et al. 2005; Hausser et al. 2000; Heckman et al. 2003; Magee and Johnston 2005; Migliore and Shepherd 2002). Spinal motoneurons have especially strong voltage-sensitive conductances in their dendrites (Hultborn et al. 2003; Lee and Heckman 2000; Prather et al. 2001). Excitatory and inhibitory synaptic inputs in motoneurons, as in other neurons, are largely located in dendritic regions (Fyffe 2001) and thus necessarily interact with dendritic voltage-sensitive channels before reaching the soma and generating spikes. Thus dendrites are active participants in synaptic integration, providing the potential not only for strong input amplification but also for highly nonlinear input interactions. Neuromodulatory input may also influence synaptic integration via the facilitation of voltage-sensitive conductances. These neuromodulatory inputs are likely to be tonically active in vivo (Aston-Jones et al. 2000; Jacobs et al. 2002; Steriade 2001). The effect of

Address for reprint requests and other correspondence: C. J. Heckman, Ward 5-295, 303 E. Chicago Ave, Chicago, IL 60611 (c-heckman@northwestern.edu).

neuromodulators on voltage-sensitive conductances is not limited to the soma but extends to the dendrites (Frick and Johnston 2005; Heckman et al. 2003). Motor output is not generated solely by excitatory input but can also involve significant levels of inhibition (Berg et al. 2007; Perreault 2002). Thus normal synaptic integration in vivo depends on the interactions of neuromodulatory input with both excitation and inhibition.

In this study, we investigate the linearity of summation of excitatory and inhibitory synaptic inputs to the dendrites of adult spinal motoneurons subject to strong neuromodulation. We use a preparation of the feline spinal cord that provides two important advantages: selective activation of ionotropic synaptic inputs, via afferents from muscles, and tonic activity in a major neuromodulatory input from the brain stem, via axons releasing the monoamines serotonin and norepinephrine (Hounsgaard et al. 1988). Our voltage-clamp technique prevents voltage-sensitive channels at the soma from influencing synaptic input, forcing the interactions between intrinsic and synaptic currents to occur in the relatively unclamped dendritic tree (Heckman and Lee 2001). Additionally, our technique also prevents synaptic input to the soma from affecting somatic voltage-sensitive channels. Voltage clamp also allows us to measure input summation as a function of voltage level at the soma to help identify sources of nonlinear interactions.

Previous studies using these methods have shown that monoaminergic input facilitates persistent inward currents (PICs) in motoneuron dendrites (Carlin et al. 2000; Hounsgaard and Kiehn 1993; Lee and Heckman 1996). Dendritic PICs amplify excitatory synaptic currents by as much as five-to tenfold (Hultborn et al. 2003; Lee and Heckman 2000; Lee et al. 2003; Prather et al. 2001). Once the cell is depolarized sufficiently to achieve full PIC amplification, a steep decline in the total excitatory current occurs in more depolarized membrane potential ranges (Lee and Heckman 2000) (see Fig. 1C). Nonetheless, two sources of excitation sum in a nearly linear fashion during repetitive firing (Prather et al. 2001). Inhibition effectively suppresses the dendritic PIC, but in a voltage range that is more depolarized than that for excitatory input. PIC suppression herefore overlaps with the range where excitatory current declines (Hyngstrom et al. 2007; Kuo et al. 2003). Our results show that nonlinear summation tended to compensate for the differences in PIC interactions with excitation and inhibition. Thus the net current due to the summation of excitation and inhibition was more consistent (i.e., varied less) as a function of membrane voltage. Because the PIC has a major effect on repetitive firing in motoneurons, this compensation and resulting consistency across membrane voltage range is likely to play a significant role in determining motor output when the motoneuron is driven by combinations of excitation and inhibition.

Methods

Surgical preparation

All surgical procedures were approved by the Northwestern University Institutional Animal Use and Care Committee. All experiments (total of 21) used the decerebrate cat preparation (for details see Lee and Heckman 1998b). The surgical preparation was completed under deep anesthesia (1.5–3% isoflurane in a 1:3 mixture of O_2 and NO_2). The right carotid artery was cannulated to monitor blood pressure and the right jugular vein was cannulated for delivery of drugs. The mixed nerves to the medial gastrocnemius and lateral gastrocnemius and soleus (MG and LGS) muscles were located and cuff electrodes were applied for antidromic identification of MG and LGS motoneurons (all experiments). Additionally, the common cutaneous sural nerve (5 experiments) and common peroneal (CP) nerve (12 experiments) were isolated and cuff electrodes applied for generating excitatory and inhibitory synaptic input to MG and LGS motoneurons. The MG and LGS (all experiments) and tibialis anterior/extensor digitorum longus tendons (TA/EDL, 11 experiments) were cut

distally and secured to a tendon vibrator. A bilateral pneumothorax was performed to promote stable recordings by lessening movement of the chest wall. A laminectomy was completed from L_3 to L_7 vertebrae to expose the spinal cord and the cord was then bathed in mineral oil. Motor thresholds were determined for MG and LGS nerves. The animal was then paralyzed with Flaxedil (120 mg initial dose, then supplemented as needed) and ventilated. In 6 of the experiments, to diminish descending monoaminergic drive from brain stem centers, the cord was spinalized at T_{10} prior to decerebration. A laminectomy was done at $T_{9,10}$ and two sutures were placed under the cord. The cord was then transected between the sutures. A precollicular decerebration was performed and all forebrain anterior to the lesion was aspirated and replaced with loosely packed saline-soaked cotton. The anesthesia was discontinued and recordings began ≥45 min after decerebration.

Electrophysiology

Intracellular recordings of lumbar motoneurons were done using sharp electrodes with resistances of 3–5 M Ω. Electrodes were filled with 2 M potassium citrate. Voltage-clamp recordings were performed using the Axoclamp 2A amplifier (Axon Instruments) in single-electrode discontinuous mode (9- to 10.5-kHz switching frequency). Due to the large current necessary to voltage clamp the motoneurons, an external feedback loop was added to increase the gain by a factor of 11 (Heckman and Lee 2001). This gain factor resulted in excellent clamp control, with deviations of <0.5 mV in voltage ramps. Voltage-clamp data were smoothed by digital filtering (−3 dB point of 0.3 kHz).

Synaptic input

Ia monosynaptic excitatory synaptic input to MG and LGS motoneurons was achieved by vibration of the Achilles tendon (180 Hz, 80 μm peak-to-peak). Muscle length was set to about 5 to 7 mm longer than slack length. This degree of stretch provides good driving of muscle spindle Ia afferents during vibration (Lee and Heckman 1996, 2000). In six experiments, polysynaptic excitatory synaptic input to MG motoneurons was generated by electrical stimulation of the caudal cutaneous sural nerve (100 Hz) (1.1–1.4 × threshold; this low intensity avoids the inhibitory component that can accompany sural input; sural input was not applied to LGS motoneurons; see LaBella et al. 1989). Reciprocal Ia inhibition to MG and LGS motoneurons was produced by 100-Hz electrical stimulation of the CP nerve at 1.2–2.0 × motor threshold or by vibration of the common TA/EDL tendon (180 Hz, 80 μm peak-to-peak). The protocol used to assess these inputs (next section) assumes that they are constant for about 5 s. Although both Ia and sural excitation exhibit a slight decay in the first 1 s of steady stimulation, current thereafter is steady for many seconds (e.g., Lee and Heckman 2000; Prather et al. 2001). Many types of inhibition to motoneurons fade rapidly to repetitive stimulation (Heckman et al. 1994; Lafleur et al. 1993a,b); this is not true of the inputs used here, which thus meet the 5-s criterion (Kuo et al. 2003; Lee and Heckman 2000).

Protocol and data analysis

MG and LGS motoneurons were first identified by antidromic stimulation of peripheral nerves. In discontinuous voltage-clamp mode, the cell was held 5–10 mV hyperpolarized to its resting potential, after which a slow (6–8 mV/s) voltage ramp was applied in the absence of synaptic input. The same ramp was repeated in the presence of excitatory and inhibitory synaptic input alone and simultaneously. A second voltage ramp with no additional synaptic input was repeated to ensure cell health was maintained. Order of synaptic inputs was varied to prevent biased effects. Effective synaptic current (I_N) was calculated by subtracting the current traces from the synaptic trials from an average of control trials. Input conductance was determined by fitting a line to the linear hyperpolarized portion of the cell's current–voltage (I–V) function. By subtracting the cell's I–V function from the line fitted to the

hyperpolarized region we were able to determine PIC amplitude. Criteria for cell acceptance included: *1*) antidromic spike height of ≥60 mV; *2*) holding current required to maintain the initial holding potential did not change >20%; *3*) control input conductance did not change >20%; *4*) the peak amplitude of the persistent inward current measured during control trials did not decline by >20%; and *5*) adequate settling of the electrode during the recording. Consistency of the PIC was the main source of measurement error. To avoid systematic effects of this error, presentation order of excitation and inhibition was varied from cell to cell. Student's *t*-test and paired *t*-test were used to make significance comparisons ($P < 0.05$) and ANCOVAs were used to compare differences in the slopes and intercepts between regression lines ($P < 0.05$). Excel and SPSS programs were used for data processing and data analysis.

Results

Synaptic and intrinsic dendritic conductances shape the current–voltage function

Synaptic integration in spinal motoneurons was studied under two states of monoaminergic drive to the cord. In the medium monoaminergic state, the cord was intact and thus subject to tonic activity from descending monoaminergic inputs that is present in the decerebrate preparation (Hounsgaard et al. 1988) [The high monoaminergic state, achieved by exogenous administration of monoaminergic agonists (Lee and Heckman 1999), was not studied here.] In the low monoaminergic state, the cord was fully transected at the thoracic level to eliminate descending monoaminergic input (Hounsgaard et al. 1988). All studies were carried out in quasi–steady-state conditions, with both excitatory and inhibitory inputs applied as steady backgrounds. The basic protocol for all cells is illustrated in Fig. 1A, using Ia excitation and Ia reciprocal inhibition (see METHODS). The current–voltage function of the cell was assessed in control conditions (dotted line), with steady backgrounds of Ia excitation (*dashed trace*) and Ia inhibition (*top thin trace*). Results for simultaneous activation of both inputs are considered later.

The PIC is evident in the control *I–V* function as a strong downward deflection, producing a negative slope region (see control trace, Fig. 1A) (Delgado-Lezama et al. 1997; Lee and Heckman 1996,1998a; Schwindt and Crill 1980). The large changes in the *I–V* function during the synaptic background conditions are due to interactions between the PIC and these synaptic inputs in dendritic regions, outside of the good voltage-clamp control applied at the soma (Heckman and Lee 2001). The asymmetry of the PIC interaction with excitation and inhibition noted in the INTRODUCTION is evident in Fig. 1A: excitation hyperpolarizes and broadens the activation of the PIC (*bottom trace*) (Lee and Heckman 2000), whereas inhibition suppresses the PIC amplitude without altering its activation voltage (Kuo et al. 2003). These differences in interaction of excitation and inhibition with the PIC are especially clear in leaked subtract *I–V* functions (Fig. 1B).

All subsequent results are derived from these basic *I–V* function protocols. In addition to Ia excitation and Ia inhibition (in 14 cells), we also used stimulation of the common cutaneous sural nerve alone ($n = 3$) and in combination with Ia excitation ($n = 3$). No significant differences were found for Ia versus sural excitation and these results were combined. We also studied Ia excitation combined with inhibition from electrical stimulation of a mixed nerve, the common peroneal (CP; $n = 11$). Both types of inhibitory inputs significantly increased input conductance ($P < 0.001$ in both cases, paired *t*-test), but the average percentage change in conductance for CP inhibition was significantly larger (Ia: 9 ± 10%; CP: 35 ± 25%; $P < 0.02$, *t*-test). Neither excitatory input significantly altered input conductance, which is consistent with previous work (Heckman and Binder 1988; Heckman et al. 1994). It should be emphasized that all sources of excitation and inhibition used in this

study produce reasonably steady currents for the duration of the voltage ramps used here (see METHODS).

Amplification of excitatory and inhibitory inputs occurs in different voltage ranges

The effective synaptic (I_N) currents generated by Ia excitation and Ia reciprocal inhibition are shown in Fig. 1C. I_N is the net current generated at the soma by a synaptic input (Heckman and Binder 1988, 1991) and can be calculated by subtracting the control I–V function in Fig. 1A from each of the steady synaptic background I–V functions (Lee and Heckman 2000). Because the ramps were applied slowly, this subtraction process closely approximates the I_N that would be generated if the membrane potential was stepped to a steady holding potential, synaptic input applied, and the change in current measured (Lee and Heckman 1996, 2000). (I_N was inverted in this study to make excitation positive and inhibition negative, simplifying presentation of summation results.) Applying both excitation and inhibition in the same cell produced results consistent with previous work in which these inputs were studied in different cell samples. The cell in Fig. 1C displays very marked amplification of excitation (+Ia I_N; Fig. 1C, *dashed trace*), with a peak around −45 mV, followed by strong reduction above −45 mV (cf. Lee and Heckman 2000). This strong decline in excitatory synaptic efficacy may be due to both strong dendritic depolarization from PIC activation as well as activation of dendritic voltage-sensitive outward currents (Lee et al. 2003; Li and Bennett 2007). The suppression of the PIC by Ia reciprocal inhibition also provides net input amplification (cf. Kuo et al. 2003), so that inhibitory Ia current (–Ia I_N) also exhibits a peak but at a more depolarized level (−38 mV compared with −45 mV for +Ia I_N; on average for the 31-cell sample this difference was 5.3 ± 3.23 mV, $P < 0.0001$, paired t-test). The overall degree of amplification was also similar to our previous work (i.e., about a threefold amplification of excitatory Ia I_N and inhibitory Ia I_N in the medium compared with low monoaminergic states; Kuo et al. 2003; Lee and Heckman 2000).

Summation of excitation and inhibition during dendritic PIC amplification

In a cell with perfect voltage and space clamp, the current generated by ionotropic synaptic inputs varies linearly with voltage and also undergoes linear summation. This linearity occurs because voltage-clamp controls the driving force for the entire membrane of the cell. In the present study, only the soma is well clamped. Therefore the amplification and saturation of synaptic input due to the dendritic PIC (Fig. 1C) may also induce nonlinear input summation in dendritic regions. In other words, the good voltage clamp at the soma (see METHODS) provides the advantage of focusing our results on the nonlinear interactions between synaptic input and the PIC in dendritic regions.

Linearity of summation was assessed by comparing the actual summed I_N, generated by simultaneous activation of both excitation and inhibition, to the summed I_N, calculated from linear addition of the I_N currents generated by independent activation of excitation and inhibition (e.g., Powers and Binder 2000). Average I_N was determined for three 5-mV voltage windows (sub-PIC, peak excitatory I_N, and peak inhibitory I_N; see Fig. 2C). Thus nonlinear summation is defined by deviations of actual from linear. Examples are shown in Fig. 2. The linear summed I_N currents (*dotted traces*) exhibited large variations in amplitude as holding potential was depolarized, with net excitation tending to dominate near the voltage for peak excitatory amplification and net inhibition at the more depolarized voltage for peak inhibition. The actual summed I_N currents (*thick traces*) exhibit deviations from the linear summed I_N currents (*dotted traces*, indicating the presence of nonlinear summation. It is evident that this nonlinear summation results in deviations both above and below the linear prediction. We have adopted the following terminology to describe these deviations. In the voltage range where peak amplification of excitatory input occurred, actual summed

I_N was less positive than the linear summed I_N, giving sublinear summation. In contrast, at the more depolarized voltage range where peak amplification of inhibition occurred, the actual summed I_N was more positive than the linear summed I_N, giving supralinear summation. The examples in Fig. 2 show the full range of nonlinear behavior, from large (Fig. 2, A and C) to moderate (Fig. 2B).

The trend for a transition from sub-to supralinear summation was consistent in the data set as a whole. Summation was quantified in three voltage windows, each 5 mV wide (see the horizontal lines in the examples in Fig. 2). Figure 3 plots actual versus predicted results for each neuron in each window. Figure 3A shows that, in the sub-PIC voltage window (centered 5–10 mV hyperpolarized to the resting potential), sublinear summation occurred in many cells, but overall this trend was not significant (actual I_N differed from predicted I_N by −0.6 ± 1.7 nA; $P = 0.064$, paired t-test). For the voltage window centered on the peak of excitatory amplification (Fig. 3B), actual I_N tended to be sublinear by an average of −1.5 ± 2.7 nA and this difference was significant ($P < 0.003$, paired t-test). In contrast, within the voltage window centered on the peak of inhibitory amplification (Fig. 3C), summation was significantly supralinear (actual more positive than predicted) (difference of +1.9 ± 3.4 nA; $P < 0.003$, paired t-test). The relative nonlinearity in each voltage window was calculated by dividing these average nonlinearities by the absolute value of the sum of the applied inputs. This procedure gave equal weight to both excitatory and inhibitory inputs. In the peak excitatory and inhibitory windows, nonlinear summation was found to be of similar magnitude, averaging 15% sublinear in the peak excitatory voltage window and 18% supralinear in the peak inhibitory window. Each of these average percentages is significantly different from zero (t-test, $P = 0.0004$ and $P = 0.0007$, respectively). In the sub-PIC window, the average of 6% was not significantly different from zero.

Figure 3 also shows that, in all voltage windows, the input combinations spanned a wide range, from inhibition being dominant (lower left quadrants) to excitation being dominant (upper right quadrants) (each data point is from a different cell). Thus our studies were not biased by a narrow range of relative amplitudes of excitation and inhibition. The amplitude of nonlinearity for each cell in Fig. 3 is indicated by the vertical distance from the line where $y = x$ (thick line). There was no tendency for nonlinear summation to increase or decrease with relative amount of inhibition versus excitation and thus linear regression satisfactorily fit data for all voltage windows. The deviations from linearity were not significantly correlated with basic motoneuron properties (e.g., input conductance) or with PIC parameters (e.g., amplitude, voltage threshold). In all three windows, the slopes of the regression relations were not significantly different from 1.0 (i.e., the 95% confidence intervals for these slopes included the $y = x$ line). We also divided the data sets according to source of input. We found no significant differences in slope or intercept for the regression relations for the data in Fig. 3 in cells where CP stimulation was the source of inhibition compared with cells with Ia inhibition, nor when sural excitation was used instead of Ia excitation (ANCOVA, $P > 0.05$ in all cases).

A striking feature of the data was the transition from sub- to supralinear summation as holding potential was depolarized from the voltage window for peak excitation to peak inhibition. To quantify the net impact of this transition, we calculated the difference between summed I_N at the voltages for peak amplification of excitation and for peak amplification of inhibition (Sum; see arrows in Fig. 2B). Overall, the transition from sub- to supralinear summation reduced Sum from 7.7 ± 4.9 nA for the linear summation case to 4.1 ± 2.9 nA in the actual case ($P < 0.0001$; for examples, see Fig. 2). Thus nonlinear summation reduced the difference in I_N between the voltage windows for peak excitatory amplification and peak inhibitory amplification. Further analysis revealed that when the linear (Sum was large (as for the cell in Fig. 2A), the nonlinear summation increased, resulting in a relatively larger

reduction in actual (Sum (again, see Fig. 2A). To illustrate this result quantitatively, Fig. 4 plots the difference between linear and actual Sum as a function of the baseline of linear Sum. A strong relationship is apparent ($r = 0.81$; $r^2 = 0.65$; $P < 0.001$). For large values of predicted Sum, the reduction in actual Sum due to nonlinear summation was substantial, as much as 10 to 15 nA (Fig. 4). Changes of these magnitudes are certainly large enough to be functionally relevant during repetitive firing (see DISCUSSION).

Summation behavior when dendritic PIC amplification is suppressed due to lack of monoaminergic input

To allow summation to be assessed without PICs, we studied cells in a preparation with minimal monoaminergic drive (acutely spinalized decerebrate; see METHODS). PIC amplitudes in these cells were found to be small [mean PIC amplitude = −3.6 ± 3.1 nA, n = 18; for the cells in the medium monoaminergic state in the previous section, mean PIC amplitude was −12.2 ± 6.4 nA; this difference is consistent with our previous studies (Kuo et al. 2003; Lee and Heckman 2000)]. The I–V functions for cells in the minimal monoaminergic state were much more linear than in the medium state, as illustrated by the example in Fig. 5A, and neither excitatory nor inhibitory I_N showed strong deviations due to amplification (Fig. 5B). Because of the general lack of clear peaks in the excitatory and inhibitory I_N currents, summation behavior was calculated in only two 5-mV-wide windows. The hyperpolarized voltage window was set 5–10 mV hyperpolarized to rest (which was similar to the sub-PIC window in the medium state). The depolarized voltage window was centered where the small PIC reached its peak value following leak subtraction. In cells with no clear PIC (as in Fig. 5), the depolarized window was placed 10–15 mV above the hyperpolarized window because this was the typical position of the PIC relative to the rest level.

Excitatory Ia I_N was small in both voltage windows (hyperpolarized window: 2.8 ± 2.2 nA; depolarized window: 4.0 ± 3.0 nA) and was not significantly different from the mean excitatory I_N measured in the sub-PIC voltage window in the medium monoaminergic state (cord intact) ($P > 0.24$). Both Ia and CP inhibition remained similar in intensity compared with the medium monoaminergic state because percentage changes in input conductance in the two states were not significantly different from each other (t-test, $P > 0.05$).

With respect to the sub-PIC voltage window in the medium monoaminergic state (Fig. 3A), summation in the hyperpolarized window in the low monoaminergic state tended to be approximately linear (square symbols, Fig. 6) (difference between observed and predicted: −0.42 ± 2.73 nA, $P > 0.5$). In the depolarized window (triangle symbols), summation tended to be slightly sublinear (difference of −1.68 ± 2.86 nA, $P < 0.03$), much as for the peak excitatory voltage window in the medium monoaminergic state (Fig. 3B). In both windows, the cells where CP stimulation was the source of inhibition tended to behave differently from the cells where Ia reciprocal inhibition was combined with excitation. For CP inhibition, the 95% confidence intervals of the slopes of the regression relations included the line $y = x$ (both windows). In contrast, regression slopes for the data with Ia inhibition were shallow and significantly <1.0 (slope = 0.39 in the subthreshold window; slope = 0.34 in the peak PIC window; in both cases the 95% confidence intervals did not include slope = 1.0). This Ia versus CP difference may be a consequence of the relative balance of excitation and inhibition. As noted in the previous section, CP inhibition tended to be stronger than Ia inhibition and thus the CP data points tend to lie in the lower left quadrant of Fig. 6, where inhibition is greater than excitation.

Discussion

The dendritic PIC has a tremendous influence on synaptic integration in motoneurons (Binder 2002; Heckman et al. 2003; Hultborn et al. 2004). Because the PIC amplification factors are two- to threefold, the dendritic PIC generates more net current at the soma (i.e., more I_N) than does the synaptic input on its own. Excitation on its own and inhibition on its own both tend to interact in a proportional manner with the PIC (Hultborn et al. 2003; Kuo et al. 2003; Prather et al. 2001). Our results revealed, however, that simultaneous activation of excitation and inhibition induced significant nonlinear summation. Furthermore, this nonlinear interaction had a very distinct form, transitioning from sublinear to supralinear as voltage-clamp holding potential was progressively depolarized. This transition compensated for an important difference in the interaction of the dendritic PIC with excitation compared with inhibition. Excitation tended to undergo maximum PIC amplification in a voltage range at which spikes would be initiated in unclamped conditions, whereas inhibition tended to be amplified at significantly more depolarized levels. The interaction between excitation and inhibition is thus inherently unbalanced, with excitation dominating in the region near spike threshold and inhibition just above (see predicted summed currents in Fig. 2, A–C). Nonlinear summation tended to restore a more consistent relation between these two inputs as membrane potential was depolarized, with this restoring effect increasing in proportion to the potential imbalance (see Fig. 4).

Possible mechanisms for nonlinear summation in the medium monoaminergic state

An important concern with any study of summation of synaptic inputs is that the input interactions may occur partially by presynaptic mechanisms. For motoneurons, interactions could occur among premotor interneurons, which are activated by the sensory afferents, or by presynaptic inhibition of afferent terminals, which is a fundamental feature of cord circuitry (Rudomin 2002). The inputs we used were selected to minimize these problems. The Ia excitation is primarily monosynaptic. A small multisynaptic component may exist, but experiments in our lab have yet to detect any effects not due to ionotropic, monosynaptic excitation (Kuo et al. 2003; Lee and Heckman 2000). Note also that the lack of amplification of Ia I_N in the low monoaminergic state indicates that this input does not significantly influence dendritic PICs by either metabotropic or *N*-methyl-D-aspartate glutamate receptors (see also Heckman et al. 2000). Ia afferents are subject to presynaptic inhibition and the cutaneous afferents activated via the electrical stimulation of the CP nerve could be a significant source of this form of inhibition (Baldissera et al. 1981). Nonetheless, presynaptic inhibition of afferents should reduce Ia and sural excitation and thus appear as a strong sublinear summation. In contrast, CP stimulation generally produced linear summation in the sub-PIC range in the low and medium monoaminergic states. Moreover, in the medium monoaminergic state, the transition from sub- to supralinear summation in the depolarized voltage windows (peak excitation and peak inhibition) indicates that presynaptic inhibition, if present, was not a dominant effect. These findings do not eliminate a role for presynaptic inhibition in our results, but do suggest that it was not large compared with other effects, such as those due to voltage-sensitive conductances. Consequently, it is likely that the dominant interactions determining linearity of summation occurred postsynaptically. Finally, it should be noted that Moritz et al. (2007) recently showed that PICs in the somatic region of motoneurons are strong and could thus amplify input (cf. Stuart and Sakmann 1995). The secure voltage clamp of the soma in the present studies, however, restricts amplification, saturation, and nonlinear interactions to regions of poor voltage control (i.e., the dendrites).

Inhibition tends to suppress the dendritic PIC (Fig. 1; Kuo et al. 2003) and thus should reduce the amplification of excitatory input. This suppression could account for sublinear summation in the voltage range for the peak excitatory I_N in the medium monoaminergic

state. Further depolarization brings on saturation of the Ia excitation when applied on its own (Fig. 1B), presumably due to dendritic depolarization or perhaps activation of voltage-sensitive outward currents. Simultaneous dendritic inhibition could provide hyperpolarization to reduce this saturation (Fig. 2) and thus result in supralinear summation.

Possible mechanisms underlying summation with minimal PIC activation

In the sub-PIC voltage window where hyperpolarization minimized the activation of the dendritic PIC by synaptic input, other voltage-sensitive conductances may still influence synaptic integration. In particular, the hyperpolarization-activated cationic current I_H, which is responsible for the "sag" to hyperpolarizing steps in motoneurons (Powers and Binder 2001), may play a significant role. Activation of I_H might offset the shunting effect of inhibition and account for the nearly linear summation seen in Fig. 3A. In the present study, such an interaction would have taken place in the poorly clamped dendritic regions. This interpretation would therefore imply that motoneurons have substantial I_H in dendritic regions, a possibility not yet investigated for motoneurons via immunohistochemical methods but supported by the experimental and modeling studies of Manuel et al. (2007).

In the low monoaminergic state, summation behavior in the hyperpolarized window was similar to that in the sub-PIC window in the medium state (i.e., approximately linear). The reason for the difference between behaviors with CP versus Ia inhibition are not clear, but dendritic I_H may again be involved. Note that in Fig. 6, the low slope for the regression relation for the Ia inhibition means that this data set tends to merge into the CP data as inhibition becomes large compared with excitation (moving toward the lower left on this plot). This trend is consistent with larger relative amounts of inhibition generating input mixtures more likely to active I_H in dendritic regions. This explanation may not be sufficient, however, in that the behavior of Ia inhibition was the same in both the hyperpolarized and depolarized voltage windows. The PIC was small enough in these low-monoaminergic-state data not to have much influence at the depolarized level, but the current injected for the somatic voltage clamp might have pushed the dendritic regions above the range of I_H activation. Further study of the effect of I_H on combinations of excitation and inhibition is warranted, especially in light of recent work with dynamic clamp showing that I_H can produce a resonant peak in synaptic current (Manuel et al. 2007).

Functional relevance of nonlinear summation of excitation and inhibition in normal motor behavior

The degree to which inhibition is actually mixed with excitation during normal motor behavior is not presently known. Berg et al. (2007) demonstrated clear comodulation of excitation and inhibition during the scratch reflex in the turtle. Although inhibition of this magnitude may not be present in other motor behaviors (see Perreault 2002), chronic recordings of spinal interneurons in the primate have shown that most of these presumably premotor cells are tonically active even in the resting state (Prut and Perlmutter 2003). These studies included interneurons with inhibitory actions on motoneurons. Thus significant inhibition may often be mixed with excitation during motor output.

Motor output is of course generated by repetitive firing in motoneurons. The voltage-clamp method used in this study had the advantage of restricting nonlinear interactions between the inputs to unclamped dendritic regions (Heckman and Lee 2001). These results are thus likely to provide key data for constraining computer simulations of dendritic processing in motoneurons, which, given the near impossibility of direct dendritic intracellular recordings in motoneurons, continue to be essential for understanding the dendritic PIC (Elbasiouny et al. 2005, 2006; Grande et al. 2007a,b). Yet our results may also be relevant to synaptic integration during repetitive firing (e.g., Prather et al. 2001, 2002). Our results in the

minimal monoaminergic state showing sublinear to linear summation of excitation and inhibition during voltage clamp are consistent with those of Powers and Binder (2000) during repetitive firing in a deeply anesthetized preparation, likely to have similarly low levels of monoaminergic drive. These similarities between firing and voltage-clamp behaviors are reasonable in that the afterhyperpolarization (AHP) that follows each spike limits the average membrane depolarization between spikes (Powers and Binder 2001). The average voltage level during firing does depolarize substantially as firing rate increases (Schwindt and Calvin 1972; Schwindt and Crill 1982), reaching the levels where excitatory saturation and inhibitory amplification occur (Lee and Heckman 1998a,b, 2000). Thus it is probable that the transition from sub- to supralinear summation seen here in voltage clamp could also produce a more consistent balance between excitation and inhibition as baseline firing rate increases from threshold levels. Consider, for example, a case where perfect linear summation prevails and where a cell is firing at a low rate, near threshold, due to a mixture of excitation and inhibition (excitation dominating, of course, or firing would not occur). As the excitatory input is increased, average membrane potential becomes depolarized, pushing the cell into the region where inhibitory amplification is greater than excitatory amplification (the peak inhibitory windows in Fig. 2). This depolarization would increase the efficacy of inhibition already present and reduce the efficacy of the added excitation, very much limiting the resulting change in firing. This limiting of the effect of excitation would be exacerbated by the decline in amplification of excitatory I_N. The nonlinear summation process, with its transition from sub- to supralinear summation, would reduce these variations in excitatory versus inhibitory synaptic efficacy and allow firing rate to increase more in proportion to the increase in net input. In general, the extra noise induced by mixing inhibition with excitation may not be a significant functional problem because the large AHP in motoneurons acts to stabilize firing rate to noisy input (Manuel et al. 2005, 2006). Overall, the processing of excitation and inhibition in motoneurons with strong dendritic PICs does involve nonlinear interactions although, to a significant degree, these nonlinearities tend to make the PIC processing of the input mixture more consistent as a function of membrane voltage.

Acknowledgments

We thank J. Miller for assistance in data collection, J. Schuster for assistance in preparation of the manuscript, and J. Kuo for assistance with data collection and technical consultation.

Grants: This work was supported by National Institute of Neurological Disorders and Stroke Grant NS-034382 to C. J. Heckman; and U.S. National Research Service Award, Predoctoral Fellowship 5F31NS048757-03, and the Foundation for Physical Therapy, Promotion of Doctoral Studies, Viva J. Erickson Scholarship to A. S. Hyngstrom.

References

Aston-Jones G, Rajkowski J, Cohen J. Locus coeruleus and regulation of behavioral flexibility and attention. Prog Brain Res. 2000; 126:165–182. [PubMed: 11105646]

Baldissera, F.; Hultborn, H.; Illert, M. Handbook of Physiology The Nervous System Motor Control. Vol. II. Bethesda, MD: Am Physiol Soc; 1981. Integration in spinal neuronal systems; p. 509-595.sect 1

Berg RW, Alaburda A, Hounsgaard J. Balanced inhibition and excitation drive spike activity in spinal half-centers. Science. 2007; 315:390–393. [PubMed: 17234950]

Binder MD. Integration of synaptic and intrinsic dendritic currents in cat spinal motoneurons. Brain Res Brain Res Rev. 2002; 40:1–8. [PubMed: 12589901]

Carlin KP, Jones KE, Jiang Z, Jordan LM, Brownstone RM. Dendritic L-type calcium currents in mouse spinal motoneurons: implications for bistability. Eur J Neurosci. 2000; 12:1635–1646. [PubMed: 10792441]

Delgado-Lezama R, Perrier JF, Nedergaard S, Svirskis G, Hounsgaard J. Metabotropic synaptic regulation of intrinsic response properties of turtle spinal motoneurones. J Physiol. 1997; 504:97–102. [PubMed: 9350621]

Elbasiouny SM, Bennett DJ, Mushahwar VK. Simulation of dendritic $Ca_V1.3$ channels in cat lumbar motoneurons: spatial distribution. J Neurophysiol. 2005; 94:3961–3974. [PubMed: 16120667]

Elbasiouny SM, Bennett DJ, Mushahwar VK. Simulation of Ca^{2+} persistent inward currents in spinal motoneurones: mode of activation and integration of synaptic inputs. J Physiol. 2006; 570:355–374. [PubMed: 16308349]

Frick A, Johnston D. Plasticity of dendritic excitability. J Neurobiol. 2005; 64:100–115. [PubMed: 15884001]

Fyffe, REW. Spinal motoneurons: synaptic inputs and receptor organization. In: Cope, TC., editor. Motor Biology of the Spinal Cord. London: CRC Press; 2001. p. 21-46.

Grande G, Bui TV, Rose PK. Effect of localized innervation of the dendritic trees of feline motoneurons on the amplification of synaptic input: a computational study. J Physiol. 2007a; 583:611–630. [PubMed: 17615105]

Grande G, Bui TV, Rose PK. Estimates of the location of L-type Ca^{2+} channels in motoneurons of different sizes: a computational study. J Neurophysiol. 2007b; 97:4023–4035. [PubMed: 17428909]

Gulledge AT, Kampa BM, Stuart GJ. Synaptic integration in dendritic trees. J Neurobiol. 2005; 64:75–90. [PubMed: 15884003]

Hausser M, Spruston N, Stuart GJ. Diversity and dynamics of dendritic signaling. Science. 2000; 290:739–744. [PubMed: 11052929]

Heckman CJ, Binder MD. Analysis of effective synaptic currents generated by homonymous Ia afferent fibers in motoneurons of the cat. J Neurophysiol. 1988; 60:1946–1966. [PubMed: 3236057]

Heckman CJ, Binder MD. Analysis of Ia-inhibitory synaptic input to cat spinal motoneurons evoked by vibration of antagonist muscles. J Neurophysiol. 1991; 66:1888–1893. [PubMed: 1812223]

Heckman, CJ.; Lee, RH. Advances in measuring active dendritic currents in spinal motoneurons *in vivo*. In: Cope, TC., editor. Motor Neurobiology of the Spinal Cord. London: CRC Press; 2001. p. 89-106.

Heckman CJ, Lee RH, Brownstone RM. Hyperexcitable dendrites in motoneurons and their neuromodulatory control during motor behavior. Trends Neurosci. 2003; 26:688–695. [PubMed: 14624854]

Heckman CJ, Miller JF, Munson M, Paul KD, Rymer WZ. Reduction in postsynaptic inhibition during maintained electrical stimulation of different nerves in the cat hindlimb. J Neurophysiol. 1994; 71:2281–2293. [PubMed: 7931517]

Heckman CJ, Theiss RD, Johnson MD, Lee RH. Active dendrites markedly enhance input-output gain in motoneurons. Soc Neurosci Abstr. 2000; 26:257–212.

Hounsgaard J, Hultborn H, Jespersen B, Kiehn O. Bistability of alpha-motoneurones in the decerebrate cat and in the acute spinal cat after intravenous 5-hydroxytryptophan. J Physiol. 1988; 405:345–367. [PubMed: 3267153]

Hounsgaard J, Kiehn O. Calcium spikes and calcium plateaux evoked by differential polarization in dendrites of turtle motoneurones in vitro. J Physiol. 1993; 468:245–259. [PubMed: 8254508]

Hultborn H, Brownstone RB, Toth TI, Gossard JP. Key mechanisms for setting the input-output gain across the motoneuron pool. Prog Brain Res. 2004; 143:77–95. [PubMed: 14653153]

Hultborn H, Denton ME, Wienecke J, Nielsen JB. Variable amplification of synaptic input to cat spinal motoneurones by dendritic persistent inward current. J Physiol. 2003; 552:945–952. [PubMed: 14500771]

Hyngstrom AS, Johnson MD, Miller JF, Heckman CJ. Intrinsic electrical properties of spinal motoneurons vary with joint angle. Nat Neurosci. 2007; 10:363–369. [PubMed: 17293858]

Jacobs BL, Martin-Cora FJ, Fornal CA. Activity of medullary serotonergic neurons in freely moving animals. Brain Res Brain Res Rev. 2002; 40:45–52. [PubMed: 12589905]

Kuo JJ, Lee RH, Johnson MD, Heckman HM, Heckman CJ. Active dendritic integration of inhibitory synaptic inputs in vivo. J Neurophysiol. 2003; 90:3617–3624. [PubMed: 12944534]

LaBella LA, Kehler JP, McCrea DA. A differential synaptic input to the motor nuclei in triceps surae from the caudal and lateral cutaneous sural nerves. J Neurophysiol. 1989; 61:291–301. [PubMed: 2918356]

Lafleur J, Zytnicki D, Horcholle-Bossavit G, Jami L. Declining inhibition elicited in cat. stimulation of group II muscle afferents. J Neurophysiol. 1993a; 70:1805–1810. [PubMed: 8294955]

Lafleur J, Zytnicki D, Horcholle-Bossavit G, Jami L. Declining inhibition in ipsi-and contralateral lumbar motoneurons during contractions of an ankle extensor muscle in the cat. J Neurophysiol. 1993b; 70:1797–1804. [PubMed: 8294954]

Lee RH, Heckman CJ. Influence of voltage-sensitive dendritic conductances on bistable firing and effective synaptic current in cat spinal motoneurons in vivo. J Neurophysiol. 1996; 76:2107–2110. [PubMed: 8890322]

Lee RH, Heckman CJ. Bistability in spinal motoneurons in vivo: systematic variations in persistent inward currents. J Neurophysiol. 1998a; 80:583–593. [PubMed: 9705452]

Lee RH, Heckman CJ. Bistability in spinal motoneurons in vivo: systematic variations in rhythmic firing patterns. J Neurophysiol. 1998b; 80:572–582. [PubMed: 9705451]

Lee RH, Heckman CJ. Enhancement of bistability in spinal motoneurons in vivo by the noradrenergic alpha1 agonist methoxamine. J Neurophysiol. 1999; 81:2164–2174. [PubMed: 10322057]

Lee RH, Heckman CJ. Adjustable amplification of synaptic input in the dendrites of spinal motoneurons in vivo. J Neurosci. 2000; 20:6734–6740. [PubMed: 10964980]

Lee RH, Kuo JJ, Jiang MC, Heckman CJ. Influence of active dendritic currents on input–output processing in spinal motoneurons in vivo. J Neurophysiol. 2003; 89:27–39. [PubMed: 12522157]

Li X, Bennett DJ. Apamin-sensitive calcium-activated potassium currents (SK) are activated by persistent calcium currents in rat motoneurons. J Neurophysiol. 2007; 97:3314–3330. [PubMed: 17360829]

Magee JC, Johnston D. Plasticity of dendritic function. Curr Opin Neurobiol. 2005; 15:334–342. [PubMed: 15922583]

Manuel M, Meunier C, Donnet M, Zytnicki D. How much afterhyperpolarization conductance is recruited by an action potential? A dynamic-clamp study in cat lumbar motoneurons. J Neurosci. 2005; 25:8917–8923. [PubMed: 16192382]

Manuel M, Meunier C, Donnet M, Zytnicki D. The afterhyperpolarization conductance exerts the same control over the gain and variability of motoneurone firing in anaesthetized cats. J Physiol. 2006; 576:873–886. [PubMed: 16931549]

Manuel M, Meunier C, Donnet M, Zytnicki D. Resonant or not, two amplification modes of proprioceptive inputs by persistent inward currents in spinal motoneurons. J Neurosci. 2007; 27:12977–12988. [PubMed: 18032671]

Migliore M, Shepherd GM. Emerging rules for the distributions of active dendritic conductances. Nat Rev Neurosci. 2002; 3:362–370. [PubMed: 11988775]

Moritz AT, Newkirk GS, Powers RK, Binder MD. Facilitation of somatic calcium channels can evoke prolonged tail currents in rat hypoglossal motoneurons. J Neurophysiol. 2007; 98:1042–1047. [PubMed: 17522175]

Perreault MC. Motoneurons have different membrane resistance during fictive scratching and weight support. J Neurosci. 2002; 22:8259–8265. [PubMed: 12223580]

Powers RK, Binder MD. Summation of effective synaptic currents and firing rate modulation in cat spinal motoneurons. J Neurophysiol. 2000; 83:483–500. [PubMed: 10634890]

Powers RK, Binder MD. Input-output functions of mammalian motoneurons. Rev Physiol Biochem Pharmacol. 2001; 143:137–263. [PubMed: 11428264]

Prather JF, Clark BD, Cope TC. Firing rate modulation of motoneurons activated by cutaneous and muscle receptor afferents in the decerebrate cat. J Neurophysiol. 2002; 88:1867–1879. [PubMed: 12364513]

Prather JF, Powers RK, Cope TC. Amplification and linear summation of synaptic effects on motoneuron firing rate. J Neurophysiol. 2001; 85:43–53. [PubMed: 11152704]

Prut Y, Perlmutter SI. Firing properties of spinal interneurons during voluntary movement. I. State-dependent regularity of firing. J Neurosci. 2003; 23:9600–9610. [PubMed: 14573540]

Rudomin P. Central control of information transmission through the intraspinal arborizations of sensory fibers examined 100 years after Ramon y Cajal. Prog Brain Res. 2002; 136:409–421. [PubMed: 12143398]

Schwindt PC, Calvin WH. Membrane potential trajectories between spikes underlying motoneuron rhythmic firing. J Neurophysiol. 1972; 35:311–325. [PubMed: 4337764]

Schwindt PC, Crill WE. Properties of a persistent inward current in normal and TEA-injected motoneurons. J Neurophysiol. 1980; 43:1700–1724. [PubMed: 6251180]

Schwindt PC, Crill WE. Factors influencing motoneuron rhythmic firing: results from a voltage-clamp study. J Neurophysiol. 1982; 48:875–890. [PubMed: 7143033]

Steriade M. Impact of network activities on neuronal properties in corticothalamic systems. J Neurophysiol. 2001; 86:1–39. [PubMed: 11431485]

Stuart G, Sakmann B. Amplification of EPSPs by axosomatic sodium channels in neocortical pyramidal neurons. Neuron. 1995; 15:1065–1076. [PubMed: 7576650]

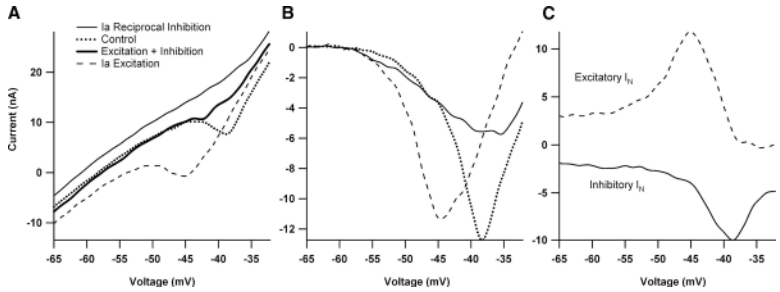

Fig. 1.

The relationship between excitatory and inhibitory synaptic input and the current-voltage *(I–V)* function. *A*: the effect of excitatory and inhibitory synaptic input applied separately and simultaneously on the shape of the persistent inward current (PIC) during a voltage ramp for one cell in the monoaminergic intact condition. All inputs were applied steadily through the duration of the *I–V* function. In the absence of additional synaptic input, the PIC appears as a downward deflection in the current profile during a voltage ramp (dotted line). Synaptic inhibition, via Ia reciprocal inhibition, causes a reduction in amplitude of the PIC (*top thin black trace*). In contrast, Ia excitatory synaptic input results in a relatively hyperpolarized PIC activation (*dashed trace*.) *B*: *I–V* functions from *A* with leak currents subtracted. The different interactions between inhibition and excitation with the PIC are evident. *C*: comparison of effective synaptic current (I_N) generated during excitatory and inhibitory synaptic input (same cell as *A*). I_N was calculated by subtracting *I–V* traces made during the application of synaptic input with traces generated during trials with no additional synaptic input (control ramps). The *dashed trace* shows the excitatory Ia I_N, which is enhanced >2-fold (compared with more hyperpolarized regions) and then decreases at more depolarized levels. The *bottom solid black trace* illustrates the inhibitory I_N, which also shows amplification, but is a result of the PIC deactivation by the Ia reciprocal inhibition. Note that peak excitatory I_N occurs at a more hyperpolarized voltage than the peak inhibitory I_N.

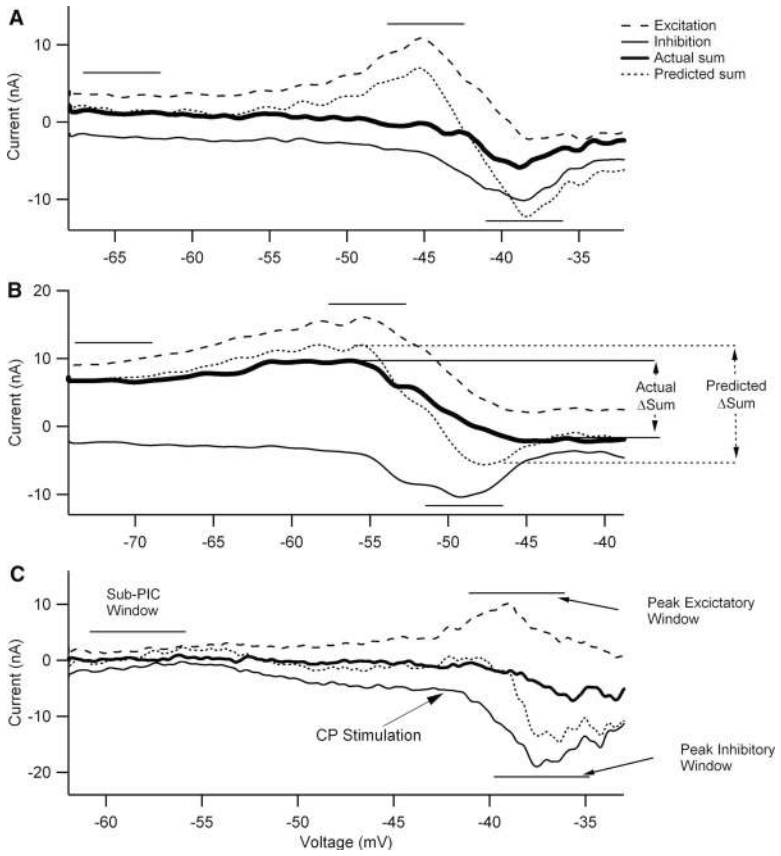

Fig. 2.

The difference in voltage onset and amplitude of peak excitatory and inhibitory I_N shapes the pattern of summation. Each cell illustrated here received excitatory (*dashed black trace*) and inhibitory (*thin black trace*) synaptic inputs applied separately and simultaneously (*thick black trace*). The I_N was calculated by subtracting stimulation trials from control trials and represents the net current measured at the soma resulting from synaptic input. In each panel, the *dashed trace* is the excitatory I_N, the *thin solid trace* is the inhibitory I_N, the *dotted trace* is the predicted sum of these two individual currents by linear addition, and the *thick trace* is the actual sum generated by simultaneous stimulation of excitation and inhibition. The horizontal lines indicate the voltage windows in which summation was assessed in each cell (see *C* for names of these windows used in the text). *A*: data for the same cell as illustrated in Fig. 1. The horizontal lines indicate the 5-mV voltage windows in which we compared the measured summation of excitatory and inhibitory I_N currents and the predicted linear summation of these synaptic inputs (sub-PIC threshold, peak excitatory I_N, and peak inhibitory I_N). *B*: a cell with an especially large PIC. As a result, both inhibitory and excitatory currents are unusually large at the hyperpolarized levels in this cell. The variable Sum is defined as the I_N difference between the peak excitatory I_N voltage window and peak inhibitory I_N voltage window. The Sum was calculated for both the actual summation trace (actual Sum) and the predicted linear summation trace (predicted Sum). *C*: a cell in which electrical stimulation of the common peroneal (CP) nerve was used to generate inhibition instead of Ia reciprocal inhibition for the cells in *B* and *C*. Note the names for the voltage windows.

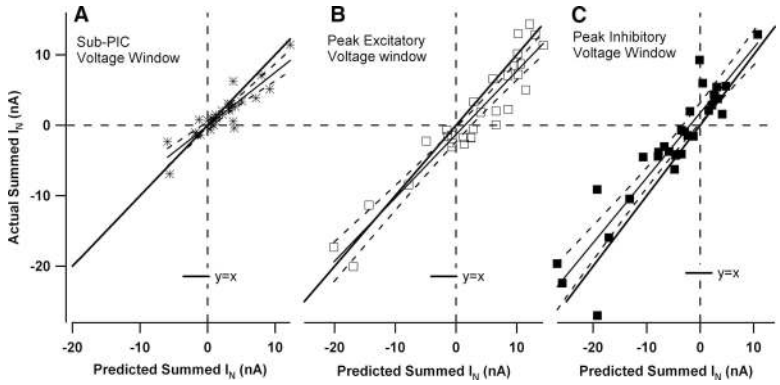

Fig. 3.

Plots of actual vs. predicted summed I_N currents for each cell in each voltage window. The actual summation of excitatory and inhibitory I_N currents was plotted against the predicted I_N for 3 voltage windows in the medium monoaminergic state: *A*: sub-PIC window ($y = 0.76x - 0.4$). *B*: peak excitatory window ($y = 0.90x - 1.3$). *C*: peak inhibitory window ($y = 0.92x + 1.74$). In each plot the thick line is a hypothetical case of linear summation where $y = x$. Vertical distance from this line represents nonlinear summation. The solid lines indicate the regression relations and the dashed lines the 95% confidence limits for the slopes.

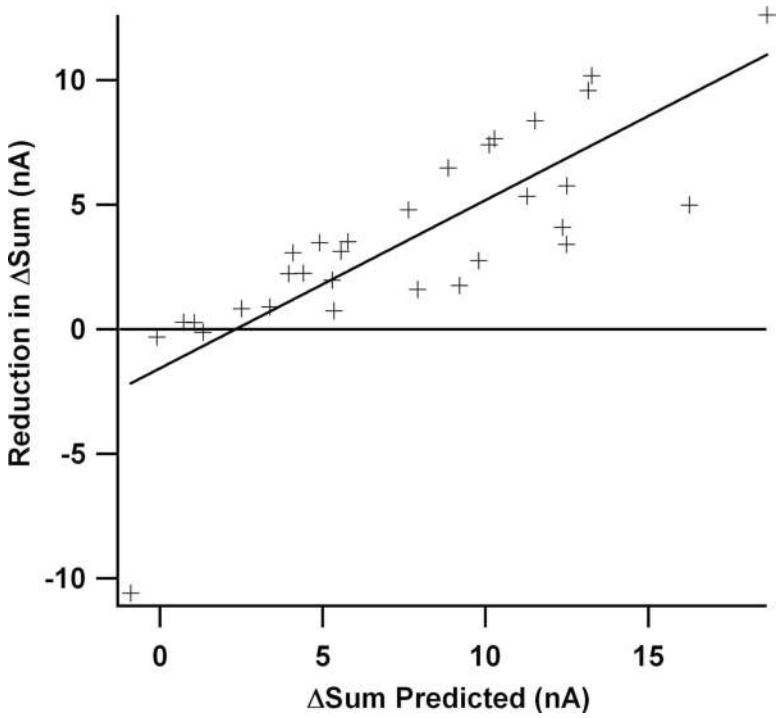

Fig. 4.

When linear addition predicts that summed I_N exhibits a large variation as membrane potential is depolarized, compensation for this variation by nonlinear summation increases. In other words, when the Sum parameter (defined in Fig. 2B) for linear summation is large, nonlinear summation markedly reduces actual Sum (as in the cell in Fig. 2A). This compensation is illustrated quantitatively by the plot shown here, where the *y*-axis is the reduction in Sum (linear Sum – actual Sum) and the *x*-axis is the baseline of linear Sum (*x*-axis) ($r = 0.81$, $r^2 = 0.65$; $P < 0.001$). This relationship is functionally relevant in that the reduction in Sum reaches currents of 10 to 15 nA (*top right*), which would modulate firing by as much as 30 Hz (cf. Lee et al. 2003).

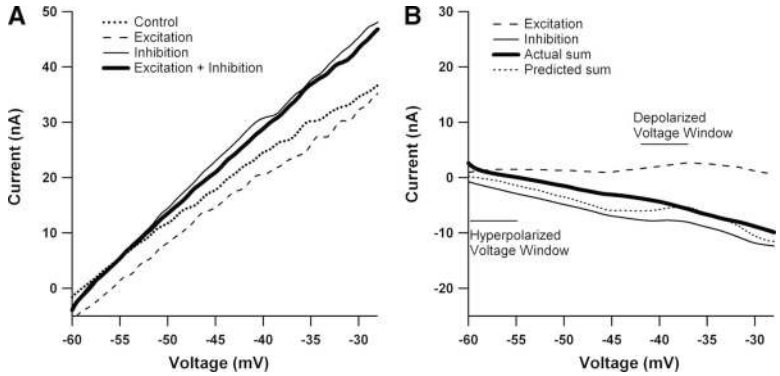

Fig. 5.

The minimal monoaminergic state results in linear *I–V* functions. *A*: current-voltage plots for one cell during control (dotted line), excitation (dashed lines), inhibition (thin black line), and excitation + inhibition (thick black line). Note the absence of any PICs (which would manifest as a negative slope region) even during the excitation trial (compare with Fig. 1A). Inhibition was applied via CP nerve stimulation and excitation by tendon vibration. *B*: due to the lack of PICs, the *I–V* relationship of the I_N currents also reveals a very linear relationship (same cell as *A*). Further evidence of decreased PIC activity is that excitation remained relatively small across voltage ranges and on average was not significantly different from the average amplitude of excitatory I_N measured in the medium state's sub-PIC voltage region ($P > 0.2$).

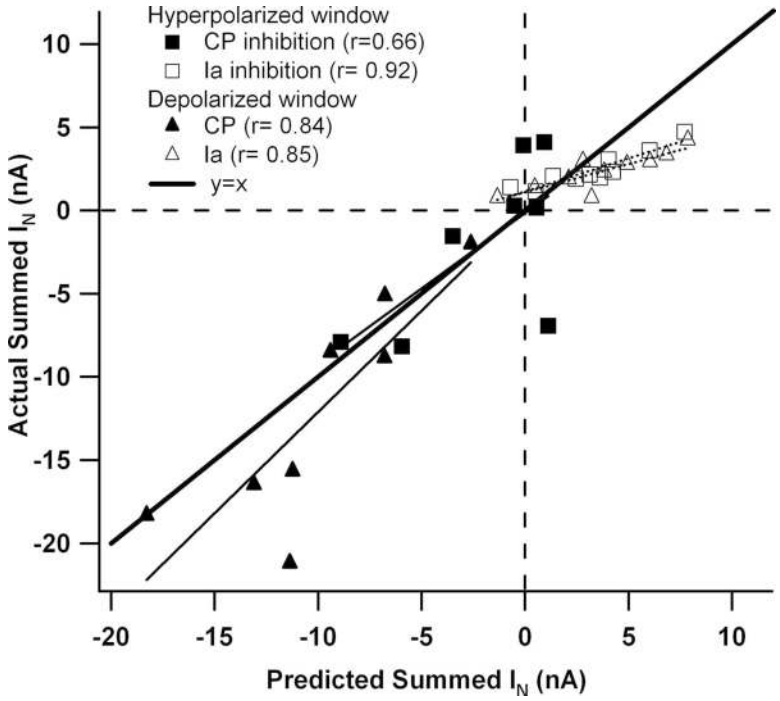

Fig. 6.

The pattern of summation in the low monoaminergic state depends on the type of stimulus. In cells where Ia inhibition and Ia excitation were combined (open symbols), regression slope was significantly <1.0 ($y = 0.39x + 1.16$ for the hyperpolarized window, open squares; $y = 0.34x + 1.09$ for the depolarized window, open triangles). The 95% confidence intervals for these slopes did not include the line $y = x$. In cells where CP inhibition was combined with Ia excitation (filled symbols), the 95% confidence intervals for regression slopes did include the $y = x$ line ($y = 0.91x + 0.14$ for the hyperpolarized window, filled squares; $y = 1.22x + 0.07$ for the depolarized window).